DØnote 5032-CONF

Measurement of the Top Quark Mass in the Dilepton Channel

The DØ Collaboration
URL http://www-d0.fnal.gov
(Dated: March 9, 2006)

We present a preliminary measurement of the top quark mass in the dilepton channel based on about 370 pb^{-1} of data collected by the DØ experiment during Run II of the Fermilab Tevatron collider. We show that the method used obtains consistent results using ensemble tests of events generated with the DØ Monte Carlo simulation. We apply our technique to the dilepton events with at least one b-tagged jet selected from the collider data to obtain $m_t = 177 \pm 12$ GeV. The statistical uncertainty is 11 GeV and the systematic uncertainty is 4 GeV.

Preliminary Results for Winter 2006 Conferences

I. INTRODUCTION

We present a measurement of the top quark mass based on about 370 pb^{-1} of data collected by the DØ experiment during Run II. The method used is similar to that used by the DØ Collaboration to measure the top quark mass in the dilepton channel using Run I data [1].

The top quark mass is an important parameter in standard model predictions. Loops involving top quarks provide the dominant radiative corrections to the value of the W boson mass, for example. Another important correction to the W boson mass originates from loops involving the Higgs boson. Thus precise measurements of the W boson and top quark masses provide a constraint on the Higgs boson mass.

The measurement in the dilepton channel is statistically limited. It provides an independent measurement of the top quark mass that can be compared with the measurement in the lepton+jets channel, and a consistency check on the $t\bar{t}$ hypothesis in the dilepton channel. With increasing data samples, the mass measurement in the dilepton channel can be performed with similar precision as that in the lepton+jets channel.

II. THE DØ DETECTOR

The DØ detector is a typical multipurpose collider detector, that consists of central tracking, calorimeter, and muon detection systems.

The magnetic central-tracking system is comprised of a silicon microstrip tracker and a scintillating fiber tracker, both located within a 2 T superconducting solenoidal magnet [2]. Central and forward preshower detectors are located just outside of the coil and in front of the calorimeters. The liquid-argon/uranium calorimeter is divided into a central section covering pseudorapidity $|\eta| \leq 1$ and two end calorimeters extending coverage to $|\eta| \leq 4$ [3]. In addition to the preshower detectors, scintillators between the calorimeter cryostats provide sampling of developing showers at $1.1 < |\eta| < 1.4$. The muon system is located outside the calorimeter and consists of a layer of tracking detectors and scintillation trigger counters before 1.8 T toroids, followed by two similar layers outside the toroids. Tracking at $|\eta| < 1$ relies on 10 cm wide drift tubes [3], while 1 cm mini-drift tubes are used at $1 < |\eta| < 2$.

The trigger and data acquisition systems are designed to accommodate the high luminosities of Run II. Based on information from tracking, calorimeter, and muon systems, the output of the first level of the trigger is used to limit the rate for accepted events to ≈1.5 kHz. At the next trigger stage, with more refined information, the rate is reduced further to ≈800 Hz. These first two levels of triggering rely mainly on hardware and firmware. The third and final level of the trigger, with access to all of the event information, uses software algorithms and a computing farm, and reduces the output rate to ≈50 Hz, which is written to tape.

III. EVENT SELECTION

The event selection was developed for the measurements of the cross section for $t\bar{t}$-production in the dilepton channel. Below, we give a simplified summary of the kinematic and topological selection cuts. The exact selection cuts are given in reference [4]. The analyses use about 370 pb^{-1} of data from $p\bar{p}$-collisions at $\sqrt{s}$=1.96 TeV collected with the DØ detector at the Fermilab Tevatron collider.

In the $e\mu$ channel, events must satisfy

- electron: $p_T(e) > 15$ GeV, $|\eta| < 1.1$ or $1.5 < |\eta| < 2.5$;
- muon: $p_T(\mu) > 15$ GeV;
- ≥ 2 jets: $p_T(j) > 20$ GeV, $|\eta| < 2.5$;
- $H_T = \max(p_T(e), p_T(\mu)) + p_T(j_1) + p_T(j_2) > 122$ GeV.

In the ee channel, events must satisfy

- two electrons: $p_T(e) > 15$ GeV, $|\eta| < 1.1$ or $1.5 < |\eta| < 2.5$;
- ≥ 2 jets: $p_T(j) > 20$ GeV, $|\eta| < 2.5$;
- $m(ee) < 80$ GeV or $m(ee) > 100$ GeV;
- $\not\!\!p_T > \begin{cases} 40 \text{ GeV} & \text{if } m(ee) < 80 \text{ GeV} \\ 35 \text{ GeV} & \text{if } m(ee) > 100 \text{ GeV} \end{cases}$;

- sphericity > 0.15.

Sphericity is defined as 1.5 times the sum of the first two eigenvalues of the normalized momentum tensor calculated using all electrons, muons and jets in the event. In the $\mu\mu$ channel, events must satisfy

- two muons: $p_T(\mu) > 15$ GeV;
- ≥ 2 jets: $p_T(j) > 20$ GeV, $|\eta| < 2.5$;
- event is inconsistent with $Z \to \mu\mu$ based on χ^2 test;
- $\Delta\phi(\mu, \not\!\!p_T) < 175^o$;
- $\not\!\!p_T > \max\left(35, 85 - \Delta\phi(\mu, \not\!\!p_T), 85 - (175 - \Delta\phi(\mu, \not\!\!p_T))\right)$ GeV.

$\Delta\phi(\mu, \not\!\!p_T)$ is the azimuthal angle between leading muon and missing p_T in degrees.

TABLE I: Expected and observed dilepton event yield from background and signal processes.

source	$t\overline{t}$	WW,WZ	Z	fake ℓ	background	total	observed
Ref. [4]	17.4 ± 1.5	1.5 ± 0.5	3.0 ± 0.6	$2.4^{+2.5}_{-1.7}$	$6.9^{+2.6}_{-1.9}$	$24.2^{+3.0}_{-2.4}$	28
untagged	15.7 ± 1.3	1.3 ± 0.4	2.5 ± 0.5	0.31 ± 0.15	4.2 ± 0.7	19.9 ± 1.5	21
b-tagged	10.0 ± 0.8	0.04 ± 0.02	0.09 ± 0.02	0.08 ± 0.11	0.21 ± 0.12	10.2 ± 0.9	14

Table I gives the expected and observed number of events. For the mass analysis we implement a few additional selection criteria. We reject events that are found to be inconsistent with the $t\overline{t}$ hypothesis because they have no solutions (see section IV). This requirement eliminates two events. In the $e\mu$ channel we further require the electron to have a value of the electron likelihood greater than 0.85. This cut eliminates the fake electron background almost entirely. The rows marked "untagged" in Table I give the expected and observed number of events after these requirements. We can essentially eliminate backgrounds by requiring at least one jet with a tight secondary vertex tag with decay length significance $\Lambda_{xy} > 7$. In all three channels b-tagging reduces the expected background fraction to less than 3%. We therefore do not apply any cut on the electron likelihood in the $e\mu$ channel. The rows marked "b-tagged" in Table I give the expected and observed number of b-tagged events.

IV. ANALYSIS TECHNIQUE

As in the Run I publication [1], we follow the ideas proposed by Dalitz and Goldstein [6] to reconstruct events from decays of top-antitop quark pairs with two charged leptons (either electrons or muons) and two or more jets in the final state. Kondo has published similar ideas [7].

We use only the two jets with the highest p_T in this analysis. We assign these two jets to the b and $\overline{b}$ quarks from the decay of the t and $\overline{t}$ quarks. If we assume a hypothesized value for the top quark mass we can determine the pairs of t and $\overline{t}$ momenta that are consistent with the observed lepton and jet momenta and missing p_T. We call a pair of top-antitop quark momenta that is consistent with the observed event a solution. We assign a weight to each solution, given by

$$w = f(x)f(\overline{x})p(E^*_\ell|m_t)p(E^*_{\overline{\ell}}|m_t),$$

where $f(x)$ is the parton distribution function for the proton for the momentum fraction x carried by the initial quark, and $f(\overline{x})$ is the corresponding value for the initial antiquark. The quantity $p(E^*_\ell|m_t)$ is the probability for the hypothesized top quark mass m_t that the lepton ℓ has the observed energy in the top quark rest frame [6].

There are two ways to assign the two jets to the b and $\overline{b}$ quarks. For each assignment of observed momenta to the final state particles, there may be up to four solutions for each hypothesized value of the top quark mass. The likelihood for each value of the top quark mass m_t is then given by the sum of the weights over all the possible solutions:

$$W_0(m_t) = \sum_{solutions} \sum_{jets} w_{ij}.$$

In the mass analysis procedure described so far we implicitly assume that all momenta are measured perfectly. The weight $W_0(m_t)$ therefore is zero if no exact solution is found. However, the probability to observe an event if the top

quark mass has the value m_t does not have to be zero if no exact solution is found, because of the finite resolution of the momentum measurements. We account for detector resolutions by repeating the weight calculation with input values for the electron and jet momenta that are drawn from normal distributions centered on the measured value with widths equal to the resolution of the momentum measurements. For muons, the inverse muon momenta are drawn from a normal distribution. The missing p_T is corrected by the vector sum of the differences in the particle momenta from the measured values and an added random noise vector with x and y-components drawn from a normal distribution with a mean of zero and an rms of 8 GeV. We then average the weight curves obtained from N such variations:

$$W(m_t) = \frac{1}{N}\sum_{n=1}^{N} W_n(m_t).$$

We thus effectively integrate the weight $W(m_t)$ over the final state parton momenta, weighted by the experimental resolutions. We refer to this procedure as resolution sampling. The main rationale for employing resolution sampling is that it increases the number of events for which we find solutions. In Monte Carlo events with an input top quark mass of 175 GeV, about 10% of the events have no solutions as measured. After sampling 1000 times for each event the fraction of events without solutions drops to less than 1%.

For each event we use the value of the hypothesized top quark mass at which $W(m_t)$ reaches its maximum as the estimator for the mass of the top quark. We call this mass value the peak mass. We cannot determine the top quark mass directly from the distribution of peak masses, because effects such as initial and final state radiation shift the most probable value of the peak mass distribution away from the actual top quark mass. We therefore generate the expected distributions of weight curve peaks for a range of top quark masses using Monte Carlo simulations. We call these distributions templates.

Monte Carlo samples were generated for nineteen values of the top quark mass between 120 and 230 GeV. The simulation uses ALPGEN [8] as the event generator, PYTHIA [9] for fragmentation and decay, and GEANT [10] for the detector simulation. The standard DØ jet energy scale corrections are applied. The scale of Monte Carlo jets is increased by 3.4% on top of the nominal jet energy scale corrections. The 3.4% correction was determined to make the invariant mass of the two jets from the W decay in lepton+jets events agree with the known W mass [11].

In order to fit the data sample we need to account for the effect of the background on the templates. We use $t\bar{t}$, $Z \to \tau\tau$, and WW events generated with the full DØ Monte Carlo and fake electron events taken from the collider data sample. We add the background distributions to the signal templates. The signal and background contributions are normalized to the expected signal-to-background ratio based on Table I. Figures 1 and 2 show the Monte Carlo templates for three different top quark masses in the $e\mu$ channel. We then compare the peak mass distribution of the observed events to these templates using a binned maximum likelihood fit.

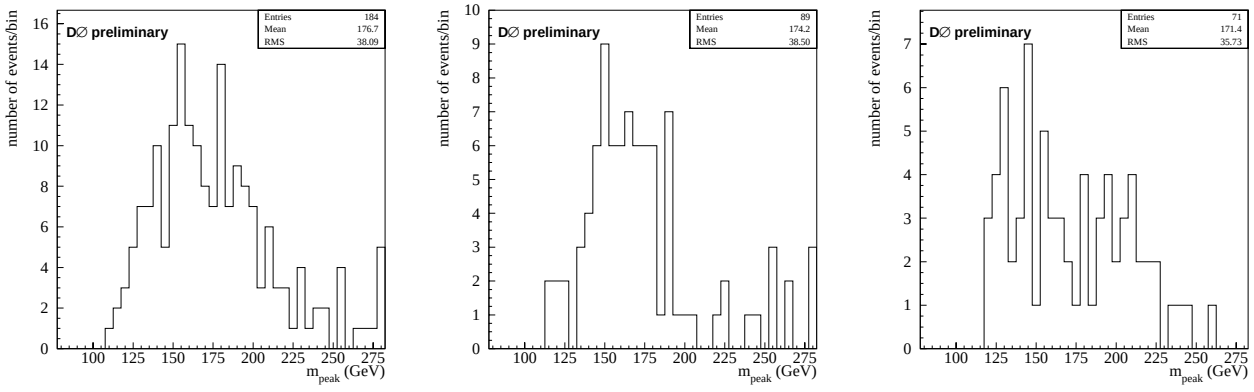

FIG. 1: Peak mass spectra for WW, $Z \to \tau\tau$, and fake electron background in the $e\mu$ channel with the untagged selection.

V. ANALYSIS OF EVENTS FROM DØ COLIDER DATA

We use the Monte Carlo templates with the nominal background contribution levels to fit the events from collider data. The joint likelihood is maximized for $m_t = 166.7 \pm 14.4$ GeV for the untagged sample and for $m_t = 178.2 \pm 11.4$

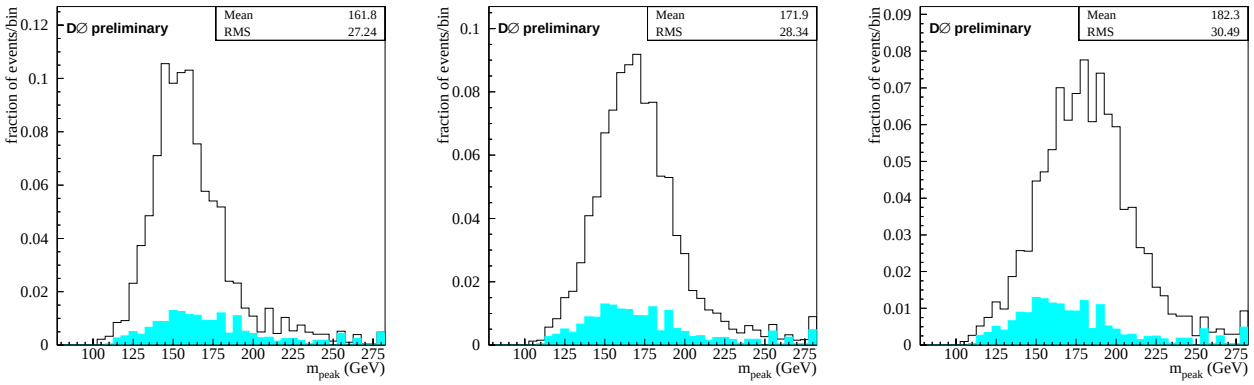

FIG. 2: Templates from Monte Carlo events from $t\bar{t}$ decays to $e\mu$ for m_t=155 GeV (left), 175 GeV (center), and 195 GeV (right) for the untagged selection. The filled histogram represents the expected background contribution.

GeV for the b-tagged sample. Figure 3 shows the joint likelihoods for all three channels for the untagged and b-tagged samples. These are computed by adding $-\ln L$ for all three channels and then fitting a quadratic function to the point with the lowest value of $-\ln L$ and its six neighbors to either side. The errors on the values of $-\ln L$ are computed by propagating the statistical uncertainties in the templates into the likelihoods.

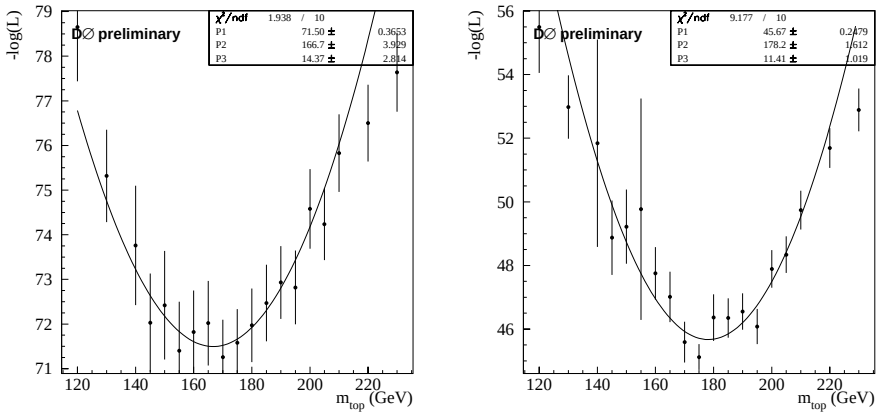

FIG. 3: Plots of $-\ln L$ versus top quark mass for the untagged sample (left) and the b-tagged sample (right).

VI. PERFORMANCE WITH DØ MONTE CARLO EVENTS

In order to demonstrate the performance of our method, we generate a large number of simulated experiments for several input top quark mass values. We refer to each of these experiments as an ensemble. We fit each of the ensembles to the templates as for collider data. The distribution of measured top quark mass values from the ensemble fits gives an estimate of the parent distribution of our measurement.

For ensemble tests events are taken from the signal and background samples with probabilities that correspond to the fraction of events expected from each sample. We calculate $-\ln L$ at every mass point separately for the three channels using the templates for the respective final state. Then we add $-\ln L$ and fit the joint likelihood versus top quark mass in the same way as for the collider data.

Tables II and III list the results of the ensemble tests, and Figures 4 and 5 show plots of average fitted mass versus input top quark mass. We fit straight lines to these points. The slope of the lines are consistent with 1.0 for both samples. The small offsets lead to corrections to the final results. In the untagged selection, the pull widths average to 0.94 and in the b-tagged selection, they average to 0.98, indicating that the error determined from the point at which

$-\ln L$ changes by half a unit slightly overestimates the statistical uncertainty. We therefore correct the statistical errors obtained from the fit by multiplying them with the respective average pull width.

TABLE II: Results of ensemble tests for the untagged analysis of 15 $e\mu$, 5 ee, and 1 $\mu\mu$ events drawn randomly from signal and background templates.

m_t	$\langle m_{fit}\rangle$	rms(m_{fit})	$\langle$pull$\rangle$	rms(pull)
150 GeV	152.5 GeV	10.0 GeV	0.25	0.96
155 GeV	156.6 GeV	8.9 GeV	0.17	0.92
160 GeV	160.2 GeV	7.9 GeV	-0.01	0.87
165 GeV	166.8 GeV	9.5 GeV	0.17	0.96
170 GeV	171.2 GeV	9.1 GeV	0.09	0.93
175 GeV	177.0 GeV	9.3 GeV	0.16	0.91
180 GeV	182.5 GeV	9.8 GeV	0.23	0.93
185 GeV	186.2 GeV	10.5 GeV	0.10	1.00
190 GeV	191.9 GeV	9.8 GeV	0.16	0.97
195 GeV	198.0 GeV	11.5 GeV	0.27	1.00

TABLE III: Results of ensemble tests for the b-tagged analysis of 10 $e\mu$, 3 ee, and 1 $\mu\mu$ events drawn randomly from signal and background templates.

m_t	$\langle m_{fit}\rangle$	rms(m_{fit})	$\langle$pull$\rangle$	rms(pull)
150 GeV	152.1 GeV	9.5 GeV	0.22	0.98
155 GeV	156.7 GeV	8.6 GeV	0.21	0.94
160 GeV	160.1 GeV	8.5 GeV	-0.02	0.93
165 GeV	167.1 GeV	8.8 GeV	0.21	0.91
170 GeV	170.6 GeV	9.3 GeV	0.02	0.99
175 GeV	175.9 GeV	9.5 GeV	0.06	1.01
180 GeV	182.1 GeV	10.0 GeV	0.19	1.00
185 GeV	187.6 GeV	10.1 GeV	0.25	0.99
190 GeV	192.5 GeV	10.8 GeV	0.22	1.07
195 GeV	196.6 GeV	9.9 GeV	0.15	1.00

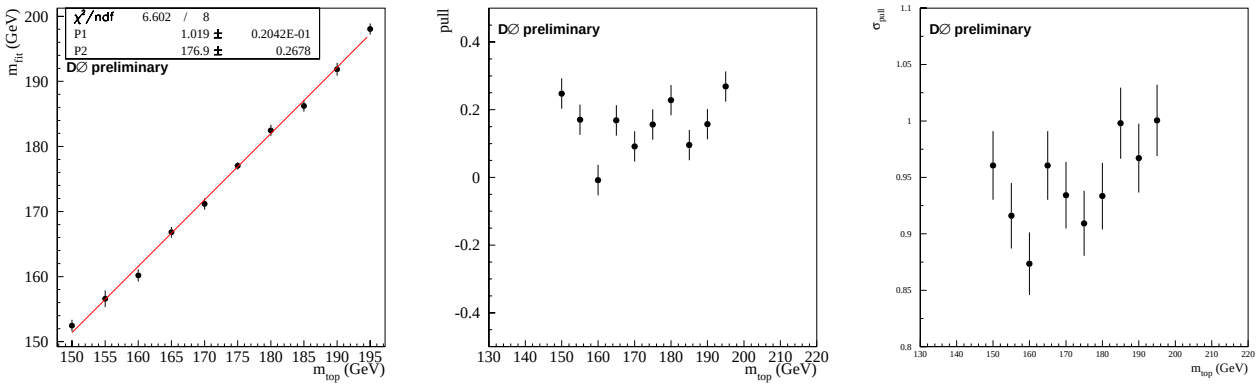

FIG. 4: Average fit mass, pull, and pull width versus input top quark mass for ensemble tests with the untagged selection.

The finite size of the Monte Carlo data samples limits the precision to which we can check the calibration of the algorithm. The systematic uncertainty is determined by the statistical errors on the mean fitted masses from the ensemble tests to be 0.3 GeV. Another source of statistical fluctuations is the limited number of ensembles (500) that we use in the calibration. In 10 sequences of 500 ensemble tests each at $m_t = 175$ GeV the results show an rms spread of 0.4 GeV. Thus the total uncertainty from Monte Carlo statistics is 0.5 GeV.

We use the ensemble test technique to study the size of the systematic uncertainties. We make systematic changes to the events in the ensembles and fit them using the nominal templates. The change in the result gives the size of the

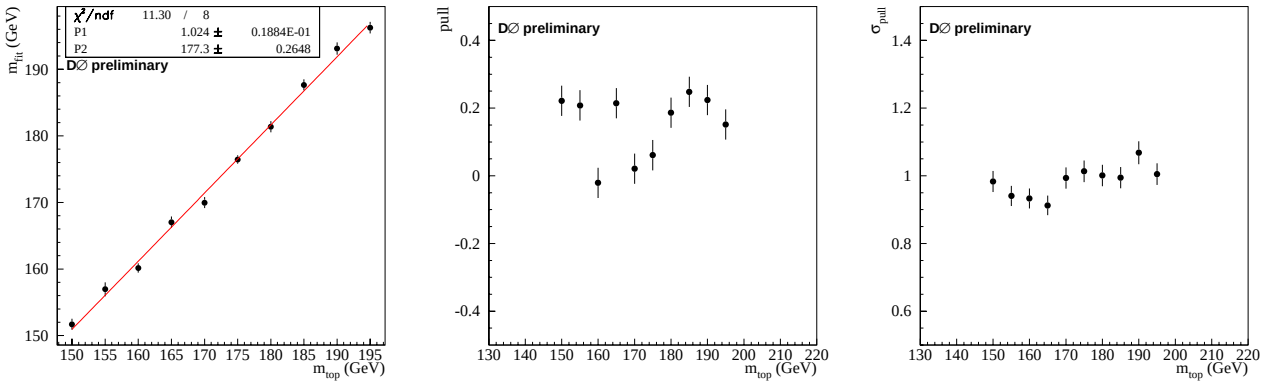

FIG. 5: Average fit mass, pull, and pull width versus input top quark mass for ensemble tests with the b-tagged selection.

systematic uncertainty. Unless noted otherwise we use the untagged selection for all three channels with the nominal backgrounds for these studies.

Since we compare the results from the collider data against simulated templates, the measurement will be systematically biased if the jet energies are calibrated differently in data and simulation. The jet energy scale uncertainty is about 4.3% which accounts for the following effects added in quadrature:

- light jet energy scale (3.5%);
- relative b-jet energy scale (1.5%);
- b-jet fragmentation (1.5%);
- p_T dependence in the jet energy scale (0.7%).
- η dependence of the jet energy scale (1.4%).

To estimate the effect of the uncertainty in the jet energy scale calibration, we generate ensembles with the p_T values of all jets decreased and increased by one standard deviation and fit them with the nominal templates. The results are shown in Fig. 6. At $m_{fit} = 165$ GeV, the average fitted mass changes by 6.7 GeV between these extremes. We quote half this difference ± 3.5 GeV as the uncertainty.

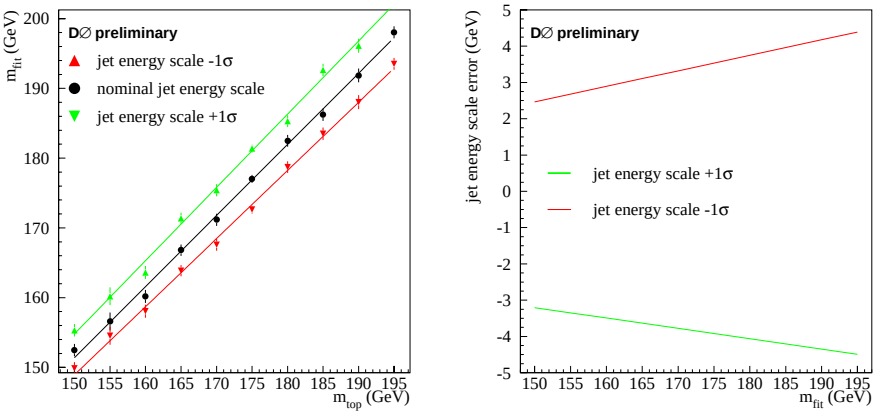

FIG. 6: Average fit mass versus input top quark mass for ensemble tests with the jet scale varied by $\pm 4.1\%$ (left). Change in top quark mass for the jet energy scale variations as a function of the fitted mass (right).

In order to estimate the effect of the uncertainty in the background estimation on the result, we increase and decrease the expected signal-to-background ratio from Table I in the ensembles by one standard deviation while keeping the nominal templates. The uncertainty is ± 0.4 GeV. The effect on the fit is shown in Fig. 7. Another limitation in the

background simulation is the small number of events. We repeat ensemble tests for $m_t = 175$ GeV 10 times, every time drawing a new background sample from Gaussian and uniform distributions that have the same mean and rms as the background templates. The results show an rms variation of 0.6 GeV which is added to the uncertainty in the untagged sample.

We repeat the variation of the background for the b-tagged sample. There is an additional uncertainty in the background estimate for the b-tagged selection that arises from the b-tagging efficiency. Since the background in the b-tagged sample is so small it is not necessary to estimate the uncertainty in the efficiency very precisely. We vary the background from zero to twice the nominal level, which changes the measured mass only by ± 0.1 GeV (see Figure 8). In addition, we add the 0.2 GeV difference between using all background events and using only b-tagged background events in the ensembles as a systematic uncertainty.

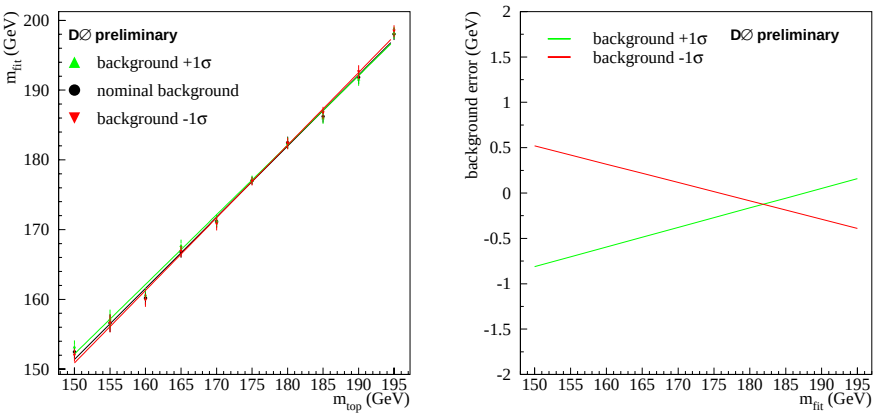

FIG. 7: Average fit mass versus input top quark mass for ensemble tests with the untagged selection and the signal fraction varied by $\pm 1\sigma$ (left). Change in top quark mass for the signal fraction variations as a function of the fitted mass (right).

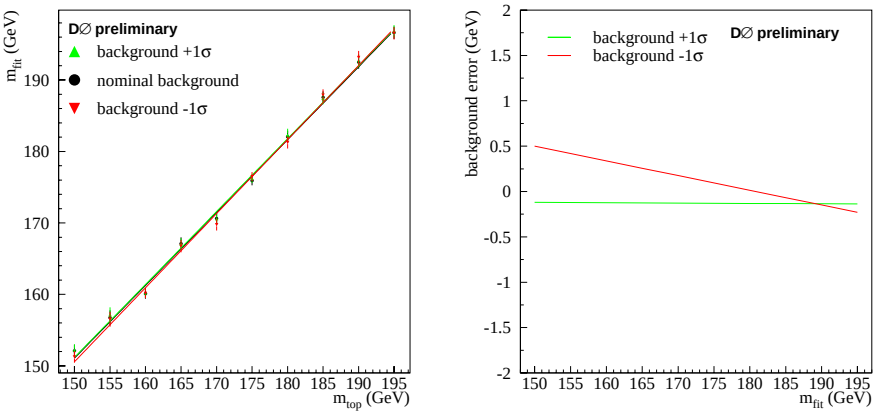

FIG. 8: Average fit mass versus input top quark mass for ensemble tests with the b-tagged selection and the signal fraction varied by $\pm 1\sigma$ (left). Change in top quark mass for the signal fraction variations as a function of the fitted mass (right).

To estimate the effect of gluon radiation on the result we study the correlation between the fitted mass and the jet multiplicity in the events. We perform ensemble tests with a varying fraction of 2-jet events in the ensembles. The results are shown in Figure 9. At fitted masses below about 180 GeV, the fitted mass decreases as the fraction of events with only 2 jets increases. Of the 21 events in our untagged data sample, 17 have only two jets and four have more than two jets. Given that we expect about four background events and 17 signal events in this sample, the observed jet multiplicity is consistent with all $t\bar{t}$ events having only two jets and with the $t\bar{t}$ events having a 2-jet fraction as small as 67%. For this range of two-jet fraction, the measured mass varies by ± 0.2 GeV. The two-jet fraction in the Monte Carlo is about 72% and thus consistent with the data. This study uses only the $e\mu$ channel without background contribution and we assume that the results can be used for all three channels.

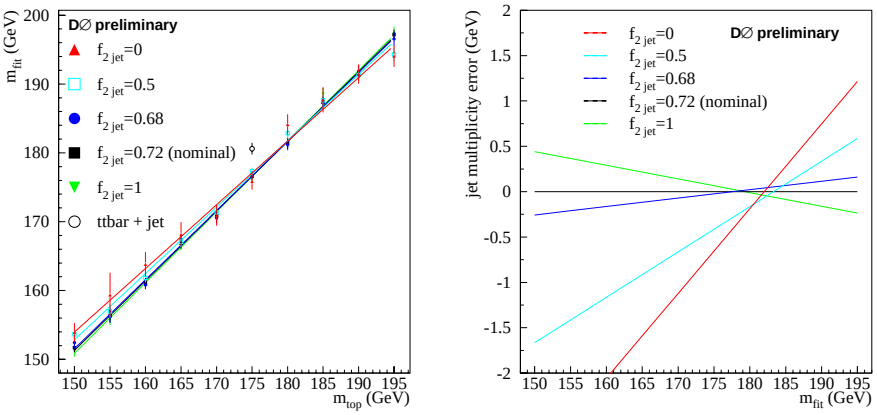

FIG. 9: Average fit mass versus input top quark mass for ensemble tests in the $e\mu$ channel with the two-jet fraction varied between 0 and 1 (left). Change in top quark mass for the variations in the two-jet fraction as a function of the fitted mass (right).

We have also generated events using the next-to-leading order event generator MCNLO [13] and HERWIG. For these events we do not use the GEANT detector simulation. In order to simulate the effects of jet reconstruction, we cluster all particles within a cone of $\Delta R = \sqrt{(\Delta\phi)^2 + (\Delta\eta)^2}$ into one "jet". Results for the samples generated with MCNLO are on average 0.8 GeV lower than using the default LO $t\bar{t}$ matrix element in HERWIG.

In the same way we used PYTHIA with varying parton distribution functions in the event generation. The spread of fitted masses observed with different parton distribution functions is 0.9 GeV [14].

VII. RESULTS

The fit results have to be corrected for the small offsets observed in the calibration (see Figure 4) and for the pull widths. The calibrated results are $m_t = 165.0 \pm 13.5(stat) \pm 3.8(syst)$ GeV for the untagged selection and $m_t = 176.6 \pm 11.2(stat) \pm 3.8(syst)$ GeV for the b-tagged selection. Table IV summarizes the uncertainties. The world average top quark mass measurement based on Run I and Run II data collected by CDF and DØ is $m_t = 172.7 \pm 2.9$ GeV [15]. Our result is perfectly consistent with the world average value.

TABLE IV: Summary of uncertainties.

source	uncertainty untagged selection	uncertainty b-tagged selection
statistical	13.5 GeV	11.2 GeV
systematic	3.8 GeV	3.8 GeV
jet energy scale	3.5 GeV	3.5 GeV
parton distribution functions	0.9 GeV	0.9 GeV
gluon radiation	0.8 GeV	0.8 GeV
background	0.7 GeV	0.2 GeV
calibration	0.6 GeV	0.6 GeV
template statistics	0.3 GeV	0.3 GeV
total	14.0 GeV	11.8 GeV

Our results with the untagged and the b-tagged selections are consistent at the level of 1.5 standard deviation. We performed ensemble tests in which we selected sets of two coupled ensembles: one with 21 events with a signal fraction of 79% and the other with 14 signal events. The two ensembles have 12 signal events in common. We then fit the two samples with templates that have the respective signal fractions. We find that the rms of the difference between the measured top quark masses in the two samples is 8.4 GeV. For two uncorrelated samples we see an rms difference of 14 GeV.

VIII. CONCLUSION

In this paper we present a preliminary measurement of the top quark mass in the dilepton channel. We show that the method used gives consistent results using ensemble tests of events generated with the DØ Monte Carlo simulation. We apply our technique to the dilepton events found in the collider data and obtain $m_t = 165 \pm 14(stat) \pm 4(syst)$ GeV $= 165 \pm 14$ GeV for the untagged selection and $m_t = 177 \pm 11(stat) \pm 4(syst)$ GeV $= 177 \pm 12$ GeV for the b-tagged selection. We obtain the more precise measurement of the top quark mass when we require the events to be b-tagged.

[1] DØ Collaboration, Phys. Rev. Letters 80, 2063 (1998); Phys. Rev. D 60, 052001 (1999).
[2] DØ Collaboration, V. Abazov *et al.*, "The Upgraded DØ Detector", submitted to Nucl. Instrum. Methods Phys. Res. A, and T. LeCompte and H.T. Diehl, Ann. Rev. Nucl. Part. Sci. **50**, 71 (2000).
[3] DØ Collaboration, S. Abachi *et al.*, Nucl. Instrum. Methods Phys. Res. A **338**, 185 (1994).
[4] DØ note 4850-CONF, "Measurement of the $t\bar{t}$ Production Cross Section at $\sqrt{s} = 1.96$ TeV in Dilepton Final States using 370 pb^{-1} of DØ Data", July 2005.
[5] DØ note 4528-CONF, "Measurement of the $t\bar{t}$ Production Cross Section at $\sqrt{s} = 1.96$ TeV in the $e\mu$ Channel Using Secondary Vertex b-tagging", August 2004.
[6] R.H. Dalitz and G.R. Goldstein, Phys Rev. D 45, 1531 (1992).
[7] K. Kondo, J. Phys. Soc. Jpn. 57, 4126 (1988); 60, 836 (1991).
[8] M.L. Mangano, M. Moretti, F. Piccinini, R. Pittau, A. Polosa, JHEP 0307:001,2003, hep-ph/0206293; M.L. Mangano, M. Moretti, R. Pittau, Nucl.Phys.B632:343-362,2002; hep-ph/0108069; F. Caravaglios, M. L. Mangano, M. Moretti, R. Pittau, Nucl.Phys.B539:215-232,1999; hep-ph/9807570.
[9] T. Sjöstrand et al., Computer Physics Commun. 135 (2001) 238.
[10] S. Agostinelli et al., Nuclear Instruments and Methods in Physics Research A506, 250 (2003).
[11] DØ note 4874-CONF "Top Quark Mass Measurement with the Matrix Element Method in the Lepton+Jets Final State at DØ Run II", July 2005.
[12] G. Corcella, I.G. Knowles, G. Marchesini, S. Moretti, K. Odagiri, P. Richardson, M.H. Seymour, B.R. Webber, hep-ph/0011363.
[13] S. Frixione, P. Nason, B.R. Webber, JHEP08(2003)007.
[14] DØ note 4725-CONF, "Top Mass Measurement in the Dilepton Channel", February 2005.
[15] The CDF and DØ Collaborations, the Tevatron Electroweak Working Group, "Combination of CDF and DØ Results on the Top-Quark Mass", hep-ex/0507091.